LEFT HAND SIDE WIND MAXIMA IN NORTH ATLANTIC AND WESTERN PACIFIC TROPICAL CYCLONES

Peter J. Sousounis , Jason Butke, and Kevin Hill*
AIR Worldwide Corporation, Boston, MA

1. MOTIVATION FOR STUDY

Most Northern Hemisphere Tropical Cyclones Have Maximum Winds on the Right

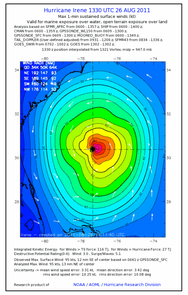

Most tropical cyclone wind fields exhibit a maximum wind speed on the right hand side (northern hemisphere – see H*WIND example of Hurricane Irene as it moves northward) which is simply the result of the tangential wind field superimposed onto the forward speed.

Extratropical transitioning (XTT), interaction with adjacent weather systems, upper level shear, and other processes can result in different wind distributions for tropical cyclones that are important to account for when forecasting landfall wind speeds and when estimating property loss.

XTT is a typical feature of storms affecting Japan and the US because these countries are located in the mid-latitudes where XTT is more common. Over 60% and nine of the top ten loss-causing events that have affected Japan undergo XTT within 500 km of the coastline. The transitioning process typically leads to the formation of fronts and in some cases the formation of strongest winds on the left hand side.

Some Have Wind Speed Maxima on the Left

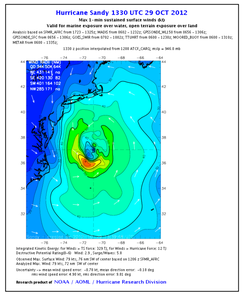

H*WIND analyses show that Hurricane Sandy exhibited strongest winds on the left hand (south) side, as it approached the New Jersey Coast – despite the high forward speed and despite the fact that strong high pressure existed to the north, which would have increased the sea-level pressure gradient on the north (right hand) side as Sandy turned northwestward towards New Jersey. In fact the strongest winds were somewhere on the left hand side for much of the trek up the East Coast of the US.

Parametric tropical cyclone risk models typically assume a wind speed maximum on the right hand side of the system (northern hemisphere). This assumption has implications when it comes to estimating a region's risk to tropical cyclone damage.

This study provides some climatological aspects that are important to understand for including tropical cyclone wind asymmetries in parametric-based risk models. Some of these aspects were studied previously by the authors but the scope was limited, only the Pacific was considered, and the methodology was different. This study provides more detail regarding the azimuthal location of the maximum wind as a function of latitude-longitude, time-of-year, and intensity and includes Atlantic and Pacific Basins.

2. METHODOLOGY

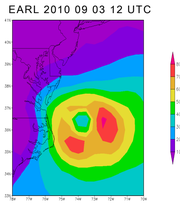

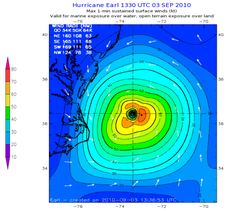

Climate Forecast System Reanalysis (CFSR) data from the period 1979-2008 was the primary data source. With 0.5° resolution and 4X daily availability it was most likely to be able to capture the locations of wind speed maxima. A CFSR example for Earl 2010 (wind speed in knots) is shown to the left as it compares to H*WIND. Track data from the Japan Meteorological Agency (JMA) for the WPAC and from the National Hurricane Center (NHC) for the NATL (HURDAT) was used to identify the positions and directions of motion for all named TC centers at six hourly times.

Surface wind speeds were obtained at 1° intervals beginning with 0.5° outward from the center to 5.5° at 15° azimuthal increments (24 different radial slices). These wind speeds were used to determine which sector (with respect to storm motion) exhibited the strongest wind speed. A Left Hand Side Maximum (LHSM) or Right Hand Side Maximum (RHSM) was identified for each track point if the strongest wind speed was found anywhere on the left hand or right hand side respectively using the above procedure. Although there was no threshold imposed for the determination of a LHSM, it was found that comparison of LHSM features across the two basins was not very sensitive to the choice of a threshold. Below are some examples of LHSMs from the reanalysis data.

* *corresponding author email: psousounis@air-worldwide.com*

3. EXAMPLES OF LEFT HAND SIDE WIND MAXIMA

ABBY 1979 12 11 06 UTC

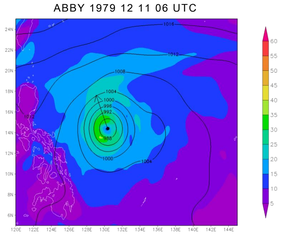

Typhoon Abby 1979 is one example from the WPAC. At the time shown the CFSR analyzed it at 985 hPa about 20 hPa higher than what JMA recorded. But, the maximum wind speeds of 35-40 m/s were very close to the 10 min sustained winds of 70 kts. Within about 500 km of The Philippines, Abby exhibited those strongest winds just to the left of straight on. This LHSM was likely the result of its heading directly towards a very strong center of high pressure (1052+ hPa) – even for that time of year.

CECIL 1979 04 13 06 UTC

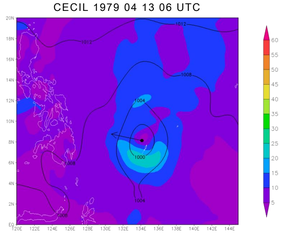

Another common type of LHSM that was identified was one like Typhoon Cecil 1979 exhibited. At the time, Cecil was still tropical storm strength equator-ward of 10N so its CFSR-analyzed central pressure was very close to the JMA central pressure. Strongest sustained winds as indicated by CFSR were clearly on the left hand side. Another characteristic of this type is the persistent nature. While many instances of LHSMs for other more northward storms were found that lasted for one or only a few six-hour periods, this one was the first of 19 consecutive 6-hourly track points to exhibit a LHSM!

BERTHA 1990 07 30 12 UTC

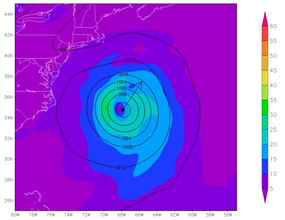

Over on the Atlantic side there were many examples of LHSMs – especially farther north in the sub-tropics or even the mid-latitudes. Presumably these were storms that were in the process of or had already undergone extra-tropical transition. Hurricane Bertha 1990 shows strongest winds over and just south of Long Island. This feature is especially significant since Bertha was moving northeastward at a fast clip and strongest winds should have been on the right.

GILBERT 1988 09 15 18 UTC

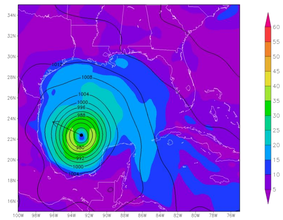

One more example for the Atlantic shows Hurricane Gilbert 1988 at still a relatively high intensity. The National Hurricane Center estimated maximum wind speeds to be 90 kts at this time. The strongest CFSR winds are about 80-90 knots off the front – on the left hand side. Large high pressure to the north does tighten the pressure gradient on the right-hand side but neither it nor the forward speed are enough to cause strongest winds on the right. Storms in proximity to the equator, particularly in the Pacific, were found to exhibit LHSMs quite frequently, as will be shown in the next panel (section).

4. DIFFERENT RESULTS BETWEEN ATLANTIC AND PACIFIC

Maximum Wind Speed Probability By Storm Relative Direction

Over 26,000 track points from the WPAC and over 10,000 track points from the NATL were analyzed. The figure to the right shows the percentage of track points with maximum wind speed relative to angle of storm motion for the two basins. On average, LHSMs were found to occur 29.37% of the time in the WPAC and 20.91% of the time in the NATL. From a relative probability standpoint, LHSMs occurred almost 50% more frequently in the WPAC than in the NATL.

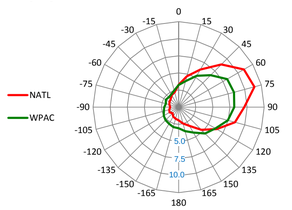

Seasonal Dependence LHSM Track Points

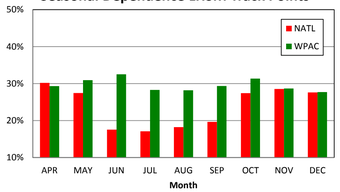

The WPAC shows much less inter-seasonal variability than the NATL. The peaks in both basins are likely attributable to XTT. Additionally, simply a higher frequency of synoptic weather systems propagating eastward through the mid-latitudes during the spring and fall seasons can enhance the SLP gradient on the western sides of TCs, which can also contribute to higher frequencies of LHSMs when the TCs begin to re-curve to the north and east.

The high percentages of LHSMs in the summer for the WPAC are curious because they are considerably higher than they are in the NATL for that time of year. This suggests some other mechanism(s) besides XTT may be responsible for the LHSMs in the Pacific that are not as present in the NATL.

Latitude Dependence LHSM Track Points

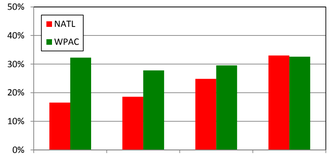

The different behavior by latitude is also noteworthy. In the NATL there is a steady increase with latitude (band). This is expected behavior and is consistent with the notion that a higher percentage of track points exhibit LHSMs as they undergo XTT. The behavior in the WPAC is very different. There is a higher percentage of LHSMs for the lowest latitude band and not much variability across latitude. Again, this result suggests that mechanism(s) other than XTT are responsible for some of the LHSMs in the Pacific.

The plots below show the track sections with LHSMs (red) and RHSMs (black) and LHSM percentages by grid cell (orange) in both NATL and WPAC basins from which can be inferred the percentages at landfall for various countries. The percentages for coastal China, the Philippines, Taiwan and Japan are comparable to the WPAC basin average. Northern China and S. Korea is lower. The percentages for the Caribbean and Florida are comparable to the NATL Basin average while those for the US East and Gulf Coasts are somewhat higher than the NATL basin average but still lower than the WPAC.

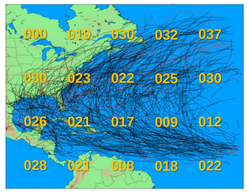

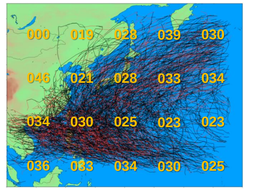

5. ROBUSTNESS OF THE RESULTS

JRA-25 – Using SLP gradients to deduce LHSMs

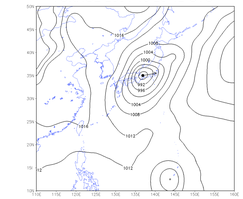

CFSR – Using Surface Wind speeds to deduce LHSMs

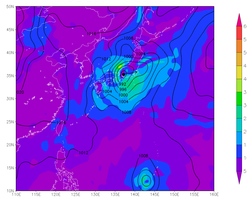

To demonstrate the robustness of the results, a different reanalysis dataset (JRA-25) as well as a different but equivalent analysis technique was used. The Japan Reanalysis (JRA-25) only exists for the period 1979-2004, so, it was supplemented with JMA Climate Data Assimilation System JCDAS data from 2005-2008 to provide a 30-year dataset. While the 1.25° resolution of the JRA-25 is sufficient for synoptic scale analyses, it is inadequate for analyzing TC wind fields. To circumvent this deficiency, a strategy that used sea-level pressure (gradients) was devised. If the SLP was highest on the LHS for a given distance from the storm center, it supported the notion that the strongest sea-level pressure gradient and hence strongest winds also existed on that side. As can be seen the difference had very little bearing on the results. An example for typhoon Tokage is shown above. The panels above illustrate the similarities between the two datasets that existed more often than not. For the JRA-25, the tighter pressure gradient on the LHS was used to determine that Tokage had a LHSM for the date and time shown.

Maximum Wind Speed Probability By Storm Relative Direction using JRA25

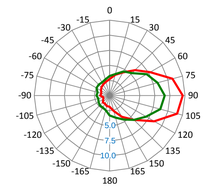

The JRA-25 result is very similar to the CFSR one. LHSMs occur 28.95% of the time in the WPAC and 20.98% of the time in the NATL. One slight difference is that the RHS JRA-25 peaks are at 90° rather than at 75°. This may be because the forward speed is not likely accounted for in the SLP distribution. In the CFSR, the surface wind speeds are earth-relative and therefore do include the forward speed component. But, it is not clear why the most likely direction is in the right-front quadrant. The percentage of LHSMs in the current study is different than that presented in our earlier study because of differences in the radial distance at which the SLP differential was analyzed and because a minimum of at least 1hPa was used in that study. The JRA-25 results were also similar to the CFSR ones in terms of seasonality and latitude (not shown).

6. SUMMARY

Specific findings include 1) WPAC TCs exhibit LHSMs with 50% higher relative frequency than their counterparts in the NATL; 2) WPAC TCs exhibit less seasonal variability with respect to LHSM frequencies than their counterparts in the NATL; 3) the WPAC exhibits a greater percentage of TCs with LHSMs at low latitudes than their counterparts in the NATL, 4) the percentage of LHSMs is highest in both basins for the highest forward speeds (not shown), and 5) significant inter-basin LHSM differences exist for relatively strong wind (>15 ms^{-1}) and strongly asymmetric situations. It is concluded that there is a fundamental difference between the activity in the WPAC and in the NATL that is responsible for the relatively higher frequency of LHSMs in the WPAC – especially in tropical latitudes, that is not associated with XTT. These results are useful for defining where the maximum wind is located as well as radial decay profiles of wind fields for certain types of stochastic events and situations in parametric-based tropical cyclone risk models.

References

Brennan, Michael J., Christopher C. Hennon, Richard D. Knabb, 2009: The Operational Use of QuikSCAT Ocean Surface Vector Winds at the National Hurricane Center. *Wea. Forecasting*, **24**, 621–645.

Chen, Y., and M. K. Yau. 2003: Asymmetric Structures in a Simulated Landfalling Hurricane. *J. Atmos. Sci.*, **60**, 2294-2312.

Frank, W. M., E. A. Ritchie, 1999: Effects of environmental flow upon tropical cyclone structure. *Mon. Wea. Rev.*, **127**, 2044–2061.

Fujibe, F., and N. Kitabatake, 2007 : Classification of surface wind fields of tropical cyclones at landfall on the Japan Main Islands, *J. Meteorol. Soc. Japan*, 85, 747-765.

Loridan, Thomas, C. S. B. Grimmond, 2012: Characterization of Energy Flux Partitioning in Urban Environments: Links with Surface Seasonal Properties. *J. Appl. Meteor. Climatol.*, **51**, 219–241.

Mueller, K. J., M. DeMaria, J. A. Knaff, J. P. Kossin, and T. H. VonderHaar, 2005: Objective Estimation of Tropical Cyclone Wind Structure from Infrared Satellite Data, *Wea. Forecasting*, **21**, 990-1005.

NOAA, 1979: NOAA Technical Report NWS 23. Meteorological Criteria for Standard Project Hurricane and Probable Maximum Hurricane Windfields, Gulf and East Coasts of the United States. U.S. Dept. Commerce, 343 pp. Available at: http://docs.lib.noaa.gov/noaa_documents/NWS/TR_NWS/TR_NWS_23.pdf.

Onogi, K., and others, 2007: The JRA-25 Reanalysis. J. Meteo. Soc. Japan, 85, 369-432. Available at: http://www.climateknowledge.org/reanalysis/Onogi_Japanese_Reanalysis_JMSJ_2007.pdf .

Powell, M. D., S. H. Houston, L. R. Amat, and N Morisseau-Leroy, 1998: The HRD real-time hurricane wind analysis system. *J. Wind Engineer. and Indust. Aerodyn.* **77&78**, 53-64

Schultz, Lori A., Daniel J. Cecil, 2009: Tropical cyclone tornadoes, 1950–2007. *Mon. Wea. Rev.*, **137**, 3471–3484.

Sousounis, P., J. J. Butke, and K. Hill, 2012: Tropical Cyclone Risk Models - Circular Symmetry Revisited. Proceedings of the 30th American Meteorological Society Conference on Hurricanes and Tropical Meteorology, Ponte Vedra Beach, Florida, April 14-20, 2012. Available at https://ams.confex.com/ams/30Hurricane/webprogram/Manuscript/Paper205892/AMS.2012.30th.Tropical.ExtAbs.PS%26J8%26KH.2.pdf .

Acknowledgements

We gratefully acknowledge the availability and use of CFSR and JRA25 Reanalysis Data for this study.

[1] AIR Worldwide (AIR) is the scientific leader and most respected provider of risk modeling software and consulting services. AIR founded the catastrophe modeling industry in 1987 and today models the risk from natural catastrophes and terrorism in more than 50 countries. More than 400 insurance, reinsurance, financial, corporate and government clients rely on AIR software and services for catastrophe risk management, insurance-linked securities, site-specific wind and seismic engineering analyses, agricultural risk management, and property replacement cost valuation. AIR is a wholly-owned subsidiary of Insurance Services Office, Inc. (ISO) .

More information is available at www.air-worldwide.com.

AIR WORLDWIDE®